Antiviral Research 103 (2014) 7–16

Contents lists available at ScienceDirect

Antiviral Research

journal homepage: www.elsevier.com/locate/antiviral

Chikungunya virus nsP3 & nsP4 interacts with HSP-90 to promote virus replication: HSP-90 inhibitors reduce CHIKV infection and inflammation *in vivo* ☆

Abhay P.S. Rathore [a,b], Timothy Haystead [c,d], Pratyush K. Das [e], Andres Merits [e], Mah-Lee Ng [b], Subhash G. Vasudevan [a,b,*]

[a] Program in Emerging Infectious Diseases, Duke-NUS Graduate Medical School, 8 College Road, Singapore 169857, Singapore
[b] Department of Microbiology, National University of Singapore, Singapore 117597, Singapore
[c] Department of Pharmacology and Cancer Biology, Duke University School of Medicine, Durham, NC 27710, United States
[d] Department of Pathology, Duke University School of Medicine, Durham, NC 27710, United States
[e] Institute of Technology, University of Tartu, Nooruse 1, 50411 Tartu, Estonia

ARTICLE INFO

Article history:
Received 1 November 2013
Revised 16 December 2013
Accepted 19 December 2013
Available online 31 December 2013

Keywords:
CHIKV nsP4
CHIKV nsP3
HSP-90
Geldanamycin
Protein interactions
CHIKV mouse model

ABSTRACT

The global emergence of Chikungunya virus (CHIKV) infection is alarming and currently there is no licensed vaccine or antiviral treatment available to mitigate this disease. CHIKV infection typically results in high viral load with an outcome of high fever, skin rashes, muscle pain, and sequelae of prolonged arthritis, which occurs in >90% of the infected cases. In this study, using biochemical pull-downs, mass-spectrometry, and microscopic imaging techniques, we have identified novel interactions between CHIKV nsP3 or nsP4 proteins with the host stress-pathway chaperone HSP-90 protein. Indeed, silencing of HSP-90 transcripts using siRNA disrupts CHIKV replication in cultured cells. Furthermore, drugs targeting HSP-90, such as commercially available geldanamycin, as well as other specific HSP-90 inhibitor drugs that had been obtained from a purinome mining approach (HS-10 and SNX-2112) showed dramatic reduction in viral titers and reduced inflammation in a CHIKV mouse model of severe infection and musculopathy. The detailed study of the underlying molecular mechanism of these viral and host protein interactions may provide a platform to develop novel therapeutics against CHIKV infection.

1. Introduction

Chikungunya virus (CHIKV) is an alphavirus that belongs to the family *Togaviridae* and is responsible for a human disease known as Chikungunya fever (Burt et al., 2012). Since its first isolation in Tanzania in 1952, CHIKV has spread massively and at present several millions of people living in Asia and Africa are at risk of contracting the disease (Schwartz and Albert, 2010). Chikungunya fever is typified by a very high viraemic load and associated abnormalities such as lymphopenia and thrombocytopenia (Borgherini et al., 2007). The disease progression is rarely asymptomatic and usually patients require medical attention, which constitutes a major socioeconomic burden on society. The mortality rates associated with CHIKV infections are low (1:1000) and the disease predominantly is self-limiting. However, in some instances patients experience a relapse with persistent arthralgia or musculoskeletal pains that can last from several months to years. Newborns and elderly people are particularly vulnerable for developing severe complications during the disease (Schwartz and Albert, 2010).

The CHIKV genome, like all alphaviruses, is a single stranded RNA molecule of ~12 kb in size and positive polarity with a 7 mG cap at the 5′ end and a poly-A tail at the 3′ end. The CHIKV genome reads in two open reading frames (ORFs), where the 5′ ORF is directly translated from the genomic RNA encodes for four non-structural proteins (nsPs) that serve various functions essential for virus replication; nsP1 contains methyl transferase and guanyl transferase activities; nsP2 is a helicase/protease enzyme; nsP3 is an accessory protein involved in viral RNA synthesis and nsP4 is the RNA dependent RNA polymerase enzyme. The 3′ ORF is translated from the 26S sub-genomic RNA and encodes for viral structural proteins such as nucleocapsid C, viral glycoproteins E1 and E2 and small peptides E3 and 6k (Li et al., 2010; Lulla et al., 2013; Strauss and Strauss, 1994; Voss et al., 2010).

☆ Parts of the information have been presented at the Keystone Conference on positive strand RNA viruses in Boston, Massachusetts, USA (April 28th–May 3rd, 2013).

* Corresponding author at: Program in Emerging Infectious Diseases, Duke-NUS Graduate Medical School, 8 College Road, Singapore 169857, Singapore. Tel.: +65 6516 6718; fax: +65 6221 2529.
E-mail address: subhash.vasudevan@duke-nus.edu.sg (S.G. Vasudevan).

0166-3542/$ - see front matter © 2013 Elsevier B.V. All rights reserved.
http://dx.doi.org/10.1016/j.antiviral.2013.12.010

To fulfill various critical functions required for virus replication, it is believed that viral non-structural proteins work in conjunction with the numerous host cellular proteins. Detailed understanding of these interactions between viral and host proteins are crucial for unraveling the viral replication and pathogenesis mechanisms and also help discover novel antiviral drug targets. In recent years various antiviral strategies have been proposed to control CHIKV infection, utilizing both viral and host targets (Kaur and Chu, 2013; Rashad et al., 2013). However, currently there is no safe antiviral treatment available to mitigate the disease. In our previous study we investigated the role of Unfolded Protein Response (UPR) machinery during CHIKV infection and showed that the UPR signaling arms such as the PERK pathway was highly regulated by viral nsP4 protein and the levels of protein folding chaperones such as HSP-90 and p58IPK were significantly induced (Rathore et al., 2013). HSP-90 has known functions in assisting the key steps of virus replication during Influenza and HCV infections (Geller et al., 2012; Okamoto et al., 2006). However, the detailed mechanism of HSP-90 involvement during CHIKV infection is not known.

In mammalian cells, HSP-90s are a family of highly conserved molecular chaperones. These include two cytoplasmic isoforms; stress-induced HSP-90α and constitutively expressed HSP-90β, the latter of which has an ER resident homologue, Grp94, and a mitochondrial homologue, TRAP-1 (Chen et al., 2005). The HSP-90 proteins form a homodimeric complex with each monomer consisting of a C-terminal dimerization domain, a middle domain and an N-terminal ATPase domain (Pearl and Prodromou, 2006). In general, HSP-90 is involved in maturation, localization, and turnover of its client proteins in a cell (Chadli et al., 2000; Prodromou et al., 2000). Viral proteins, like cellular proteins, also require folding and assembly for function and HSP-90 has been known to play an important role in the replication of many DNA and RNA viruses. For instance, HSP-90 stabilizes and stimulates the reverse transcription reaction step during hepatitis-B virus replication (Hu and Anselmo, 2000; Hu et al., 1997). Similarly, during influenza virus replication, the polymerase complex comprising of PB1, PB2, and PA is stabilized by HSP-90 protein, an essential step for virus replication (Momose et al., 2002; Naito et al., 2007). Other viruses which utilize HSP-90 proteins during their replication include alpha-herpes simplex virus-1, human cytomegalovirus, flock house virus, vesicular stomatitis virus, human parainfluenza 2/3 virus, hepatitis C virus, simian virus 5/41, and bunyavirus (Geller et al., 2012). The reliance of many viruses on HSP-90 for replication makes it an interesting potential broad-spectrum antiviral drug target. Inhibitors of HSP-90 such as geldanamycin and its derivatives, 17-allyl-17-demethoxygeldanamycin (17AAG) and 17-desmethoxy-17-N,N-dimethylaminoethylaminogeldanamycin (17DMAG) have been shown to possess antiviral activity in cell culture against range of DNA and RNA viruses (Geller et al., 2012). In this study, we evaluated both *in vitro* and *in vivo* activities of specific HSP-90 inhibitor drugs, HS-10 and SNX-2112 against CHIKV infection. Moreover, using biochemical techniques and by overexpressing individual CHIKV non-structural proteins we identified novel interactions between the HSP-90 protein and CHIKV nsP3 and nsP4 proteins. This study suggests an important role for HSP-90 during CHIKV infection and opens up the possibility of targeting this specific interaction.

2. Materials and methods

2.1. Cells and viruses

Mosquito cells *Aedesalbopictus* clone (C6/36) and baby hamster kidney cells (BHK-21) were cultured in RPMI-1640 medium (Gibco) supplemented with 10% fetal bovine serum (FBS) (Gibco). Human embryonic kidney cells expressing SV40 large T antigen (HEK-293T) were cultured in DMEM (Gibco) supplemented with 10% FBS. C6/36 cells were used for making virus stocks, grown and maintained in 28 °C temperature incubator. BHK-21 and HEK-293T cells were grown and maintained at 37 °C in a humidified incubator with 5% CO_2 atmosphere. CHIKV laboratory strain 'ROSS' and a human clinical isolate-CHIKV EAS (East African lineage strain-DMERI09/08) was a generous gift from Dr. Ooi Eng Eong (Duke-NUS reference laboratory). Viruses were amplified in C6/36 cells supplemented with 5% FBS at 28 °C and titrated by plaque assay as described previously (Rathore et al., 2011). Low passage number virus (below passage 5) was used for performing all experiments.

2.2. Therapeutic drugs

Geldanamycin was purchased from Sigma. HSP-90 inhibitor drugs; HS-10 (HS-100010) and SNX-2112 were synthesized in the laboratory of Dr. Timothy Haystead at Duke University as described elsewhere (Huang et al., 2009; Hughes et al., 2012).

2.3. Anti-CHIKV antibodies

A rabbit anti-CHIKV E1 polyclonal serum was prepared in-house. Anti-CHIKV-nsP3 and nsP4 polyclonal serum was raised and characterized in the laboratory of Dr. Andres Merits.

2.4. Cell viability

The cytotoxicity of each test drug was separately measured on BHK-21 or HEK-293T cells using the cell titer-Glo luminescent cell viability assay, according to the manufacturer's protocol (G7570; Promega). The luminescence signals for cells treated with the test drugs were compared to those for cells treated with the maximum tolerated dimethyl sulfoxide (DMSO) to determine the 50% cytotoxic concentration (CC_{50}). Furthermore, the cytotoxicity data presented in Fig. 1 was determined by counting the number of viable cells in the presence of drugs or DMSO at 24 h post-infection/treatment.

2.5. CHIKV infection of HEK-293T or BHK-21 cells

The infections of HEK-293T or BHK-21 cells were done using multiplicity of infection (MOI) of 1 of CHIKV-ROSS strain at 37 °C in a humidified incubator with 5% CO_2 atmosphere for 1 h. Cells were washed twice with non-serum containing growth media before mock or drug treatment for 12 or 24 h.

2.6. RNA extraction and real-time RT-PCR analysis

HEK-293T cells (1×10^5) were infected with CHIKV at a MOI of 1. At indicated time intervals, total RNA was extracted using the trizol (Invitrogen) extraction method and 1 μg of total RNA was used for cDNA synthesis using ImProm II reverse transcription system (Promega), with oligo-dT as primers. cDNA (50 ng) was used for real-time amplification of specific genes using respective primers (Supplementary material) in a Bio-Rad iQ-5 real time thermal cycler. The expression of viral and host gene products was normalized to actin or 18S rRNA, followed by normalization to the expression levels at uninfected conditions.

2.7. Western blotting

HEK-293T cells (1×10^5) were infected with MOI of 1 with CHIKV and total cell lysate was collected in NET lysis buffer

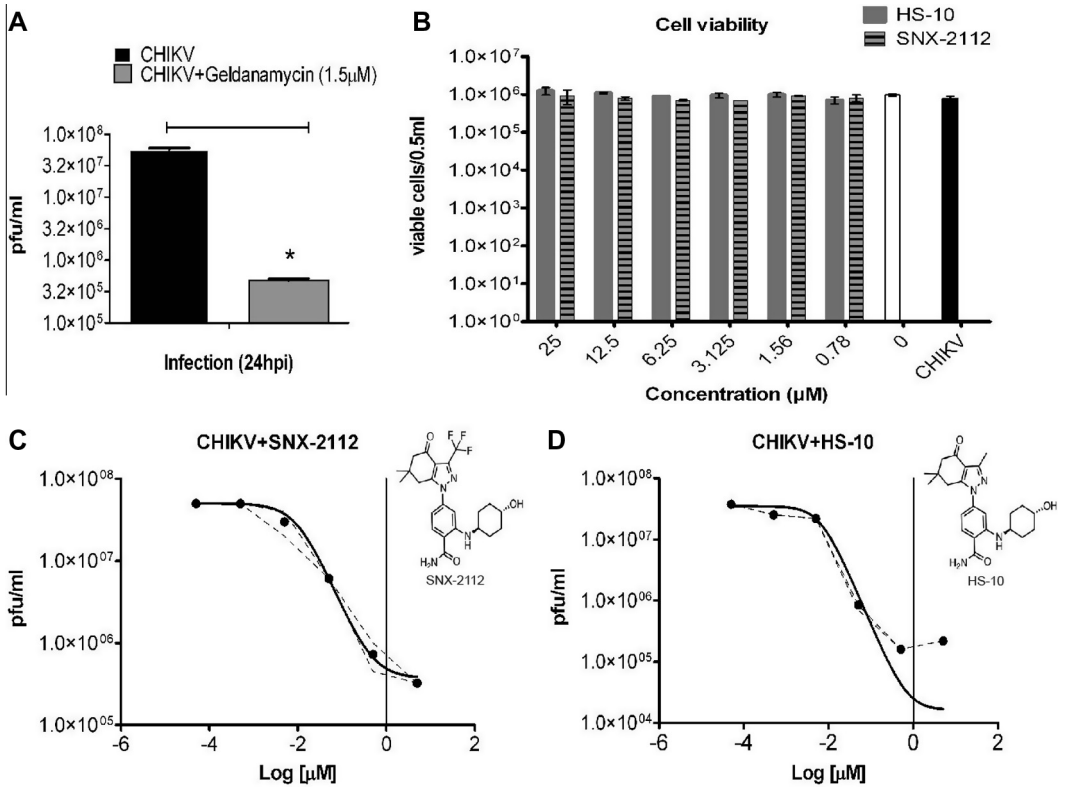

Fig. 1. HSP-90 inhibitors reduce CHIKV infection. (A) Plaque assay quantification of CHIKV replication in HEK-293T cells infected with MOI-1 of CHIKV for 1 h followed by mock or geldanamycin (1.5 μM) treatment for 24 h. At 24 h post treatment plaque assay was performed using media supernatants. (B) Toxicity test for specific HSP-90 inhibitors HS-10 or SNX-2112 in HEK-293T cells treated with increasing concentrations of drugs for 24 h followed by viable cell counting using trypan blue stain. (C and D) Dose–response curve for HS-10 or SNX-2112 in HEK-293T cells infected with MOI-1 of CHIKV for 1 h followed by mock or drug treatments at indicated concentrations for 24 h. At 24 h post treatments plaque assay was performed using media supernatant from each condition tested. A sigmoidal dose–response curve was plot using GraphPad-prism software, where dotted line represents the error range at each concentration tested.

(20 mM Tris, 100 mM NaCl & 1 mM EDTA) containing 0.1% Triton x-100 with protease inhibitor cocktail (Roche) at indicated time points post infections. After 30 min on ice, lysates were centrifuged at 13,000 rpm for 10 min and supernatants were used to quantitate the amount of total protein by BCA assay (Pierce). Equal amounts (2–5 μg each) of protein were loaded on 12% SDS–PAGE followed by Western blotting. Blots were blocked overnight with blocking solution [2% Fish gelatin (Sigma) in 1×-PBS] and were probed using primary antibodies against various proteins: CHIKV-E protein (in-house) anti-CHIKV-nsP3 serum, anti-CHIKV-nsP4 serum, total HSP-90 protein (cell signaling), HSP-90α or HSP-90β subunit (Singapore Advanced Biologics (SABIO) Pte Ltd), anti-GFP (Abcam) and anti-Actin antibody (Sigma) were used as the loading control antibodies. All the antibodies used were diluted in blocking solution. After incubating with secondary HRP-conjugated antibodies, blots were developed using ECL detection reagent (GE healthcare) and visualized using an Image-quant chemiluminescent machine.

2.8. Transfection of plasmids

For the transfection of plasmid DNA into HEK-293T cells, cells were seeded to 70% confluency in a 24 well plate (Nunc) and incubated overnight in a 37 °C incubator supplemented with 5% CO_2 atmosphere. One or 2 μg of each of the plasmid (GFP vector, GFP-CHIKV nsP1/2/3/4, described previously in (Rathore et al., 2013)) were transfected using the jet-prime transfection reagent (Polypus BST scientific) as per the manufacturers described protocol. Transfected cells were incubated for 24 h for protein expression and then washed once with 1×-PBS (Gibco). Finally, cells were collected in TNET-lysis buffer and then subjected to Western blotting as described above. The transfection efficiencies were verified by fluorescence microscopic visualization for each of the transfected plasmids.

For siRNA transfections, 100 nM each of the non-targeted, si-HSP-90(1) and si-HSP-90(2) (SABIO) were transfected in 24 well-plates using jet-prime transfection reagent (Polypus BST scientific) essentially following the manufacturers protocol. At 24 h post silencing, cells were either mock or CHIKV infected for a further 24 h. The siRNA sequences are provided in the Supplemental material.

2.9. Co-immunoprecipitation

HEK-293T cells (1×10^5) were transfected with plasmids (GFP vector, GFP-CHIKV nsP1/2/3/4) as described above or infected with CHIKV-ROSS (MOI-1) and incubated for 24 h in a humidified CO_2 incubator at 37 °C. At 24 h post-transfection, cells were washed once with 1×-PBS and lysed using TNET lysis buffer containing protease inhibitor cocktail. Lysis was continued on ice for a further 1 h with intermittent mixing at 15 min each. The cell lysates were clarified at high speed (14,000 rpm and 4 °C) and the supernatants were collected on ice. Two μg of the polyclonal anti-GFP antibody (Abcam) or HSP-90α or HSP-90β antibody (SABIO) were added in each of the clarified lysates with further incubation overnight at 4 °C with a constant mixing using an end-over-end rotor. Immune complexes formed were pulled out using 50 μl/reaction of protein A/G beads (Pierce). Finally, beads were washed 3-times with lysis buffer followed by elution of immune complexes in 1×-SDS load-

ing dye with 15 min boiling in a water bath. Eluted samples were spun at high speed before being analyzed by SDS–PAGE and Western blotting.

2.10. Sample preparation for mass-spectrometry

HEK-293T cells (5×10^6) were transfected with 10 μg of each of the plasmids (GFP, GFP-nsP3 or GFP-nsP4) for 24 h. All the steps described below were performed at 4 °C. For each immunoprecipitation reaction, cells were suspended in 200 μl of lysis buffer (10 mM Tris/Cl, pH 7.5; 150 mM NaCl; 0.5 mM EDTA; 0.5% NP-40 and complete protease inhibitor cocktail). Lysis was further continued for 30 min with extensive mixing, before lysates were being clarified at 20,000*g* for 10 min. Supernatants were collected in a pre-cooled tube and the final volume was adjusted to 0.5 ml with dilution buffer (10 mM Tris/Cl, pH 7.5; 150 mM NaCl; 0.5 mM EDTA and complete protease inhibitor cocktail). GFP-TrapA beads (30 μl each) were equilibrated in 0.5 ml dilution buffer for 15 min. Clarified cell lysates were added to equilibrated GFP-TrapA beads and were incubated under constant mixing for overnight. Beads were spun down at 2500*g* for 2 min and washed once with 0.5 ml ice-cold wash buffer (10 mM Tris/Cl, pH 7.5; 150 mM NaCl; 0.5 mM EDTA) and one time with 0.5% NP-40 in PBS followed by a final 2 washes with 50 mM ammonium bicarbonate. Elution was done using 60 μl of mass-spectrometry compatible elution buffer (0.25% RapiGest SF in 50 mM ammonium bicarbonate) and in-solution mass-spec analysis of the trypsin-digested protein samples was done using LC/ESI/MS/MS mass-spectrometry at the Duke proteomic facility, USA. Peptide sequences from the mass-spec analysis were matched against Swiss-prot 2013x database using 'Mascot' database search algorithm and the data analysis was carried out using 'Scaffold' version 4.0.7 software using peptide threshold of min 97% and protein threshold of min 45% (minimum two peptides) (Bodnar et al., 2003).

2.11. Immunofluorescence

HEK-293T cells or BHK-21 cells were seeded on glass coverslips at a density of 1×10^5 cells/well in a 12-well plate. Following incubation overnight at 37 °C with 5% CO_2, the cells were transfected with plasmids (GFP vector, GFP-CHIKV nsP1/2/3/4) or infected with CHIKV-ROSS (MOI-1). At 24 h post-transfection/infection, cells were fixed with ice cold 80% acetone for 10 min followed by overnight incubation with blocking buffer (5% BSA in 1×-PBS) at 4 °C. The primary antibodies used were anti HSP-90-total (cell signaling) or HSP-90α or HSP-90β (SABIO). The secondary antibody used was anti-rabbit alexa-594 or anti mouse alexa-488. All the antibodies used were diluted in blocking buffer. The coverslips were mounted on glass slides using prolong gold anti-fade mounting medium (Invitrogen) containing DAPI. Immunofluorescence images were captured using an upright confocal microscope (Zeiss) and image analysis was performed with Zeiss image analysis software.

2.12. In vivo infection

Sv/129 mice deficient in type -I IFN receptors (A129), purchased from B&K Universal (UK), were housed in the BSL-2 animal facility at Duke-NUS, Singapore and all animal experiments were approved by the Animal Care Committee at Singapore General Hospital. For infection, mice ($n = 6$) were inoculated with CHIKV EAS (100 pfu/20 μl) via the footpad route and the control groups were given 5% DMSO in saline as either vehicle control or mock treatment. For treatment during infection, mice were either mock or HS-10/SNX-2112 treated (10 mg/kg/twice a day) for 3 days, starting from day 0. Blood was collected for viremia at day 2 (~48 h) and 3 (~72 h) post infection/treatment. Animals were euthanized at humane end points and muscle tissues were collected for cryo-sectioning, staining and microscopic visualizations.

Limb swelling measurements: For measuring swelling in the infected limbs, animals were very briefly held in the restrainer and the measurement was done using a standard surgical ruler.

Tissue processing: Muscle tissues were harvested and frozen in OCT compound (Tissue-Tek), and frozen sectioned (~10 μm thickness) using a cryostat (Leica). Sections were fixed with acetone at 4 °C and air dried before being stained with 0.1% Mayer's Hematoxylin (Sigma) for 10 min followed by 5 min wash with water. Sections were further stained with 0.5% Eosin for 2 min, washed with water and then sequentially dehydrated using 50%, 70%, 95%, and 100% ethanol followed by final dehydration step in xylene. Slides were mounted with permount (Bio-world) before visualization and image capturing using an inverted fluorescence microscope (Olympus IX71, USA).

2.13. Serum cytokine levels

Equal volumes of serum from individual mice were pooled in each of the experimental groups and the concentration of each pro-inflammatory cytokines in the serum was measured using ELISA kits (R&D systems), following the manufacturer's described protocol.

2.14. Statistics

Statistical comparison of results were performed using unpaired Student's *t*-test using GraphPad Prism 5.0 software or using Microsoft Excel software with $p < 0.005$ considered statistically significant. For more than two comparisons one-way ANOVA test was used.

3. Results

3.1. Drugs targeting HSP-90 reduce CHIKV infection

To determine the role of HSP-90 during CHIKV infection we firstly used a commercially available, HSP-90 inhibitor drug 'geldanamycin'. Geldanamycin binds in the ATP binding site on HSP-90 and renders the protein in an open conformation (Stebbins et al., 1997). However, the ATP-driven closed conformation of HSP-90 is required for its chaperone function (Ali et al., 2006). HEK-293T cells were infected with CHIKV (MOI-1) for 1 h followed by mock or geldanamycin treatment for 24 h and virus production in the cells was monitored by plaque assay. We found that geldanamycin treatment reduced CHIKV infection by ~2.5 log suggesting a significant involvement of HSP-90 during CHIKV infectionor replication (Fig. 1A). Indeed, to rule out the possibility of any off-target effects of geldanamycin during CHIKV infection, we employed two very specific synthetic inhibitors of HSP-90, HS-10, and SNX-2112, that are close structural analogs of the clinical candidate SNX-5422 (Fadden et al., 2010). First we confirmed that the drug concentrations used in this study are not toxic to the cells (Fig. 1B). Furthermore, no cytotoxicity was observed for either of the test drugs up to 100 μM for 24 h post-drug treatments (Fig. S1). Next, we measured the efficacy of HS-10 and SNX-2112 test drugs against CHIKV infection. For this, CHIKV infected HEK-293T cells were treated at various concentrations of HS-10 or SNX-2112 for 24 h and the virus infection was measured by plaque assay. Both HS-10 and SNX-2112 showed a dose-dependent reduction in viral titers, further implicating a specific role of HSP-90 during the CHIKV infection cycle (Fig. 1C and D).

3.2. HSP-90 inhibitors affect CHIKV replication

Next, we sought to understand if the inhibitory effects seen with HSP-90 inhibitors have any direct effect on CHIKV replication. For this, HEK-293T cells were infected with MOI-1 of CHIKV followed by mock treatment or drug treatment with 10 μM dose of HS-10 or SNX-2112 for 12 h. At 12 h post infection/treatment, the amount of viral RNA (nsP1 or E2 gene) or total HSP-90 mRNA was measured by real time RT-PCR and the protein levels were measured by Western blotting (Fig. 2). Interestingly, a significant reduction (~50–100 fold) in the levels of viral RNA was observed during both HS-10 and SNX-2112 treatments (Fig. 2A and C); however, the mRNA levels of HSP-90 were not altered (Fig. 2B and C). Similarly, viral protein levels measured by Western blot detection of the CHIKV-E1 protein were also dramatically reduced during drug treatments with no significant change in the levels of total HSP-90protein (Fig. 2D). Furthermore, using immunofluorescence microscopy we observed a visually striking reduction in virus infection upon HS-10 or SNX-2112 (2 μM) treatment for 12 h (Fig. 2E). Together our data suggest that blocking the chaperone function of HSP-90 does not affect its protein level or its transcription, but, results in a marked, early (12 h) reduction in the levels of both viral RNA and protein. This early inhibition of CHIKV infection could be due to the effects of HS-10 or SNX-2112 at virus replication level.

3.3. siRNA silencing of HSP-90 has detrimental effects on CHIKV replication

To better understand the importance of HSP-90 protein during CHIKV replication, we silenced the HSP-90 transcripts using two specific siRNAs targeting the HSP-90mRNA and measured the CHIKV replication in HSP-90-knockdown cells. First, we confirmed using real time PCR that the siRNAs successfully knocked-down the transcription of HSP-90 at 24 h and noted that siRNA(2) showed more pronounced knockdown of HSP-90 and also a greater reduction in HSP-90 protein level compared to siRNA(1) or non-targeted siRNA control (Fig. 3B and C). Next, to assess the effects of HSP-90 knockdown on CHIKV replication, we infected HSP-90-knockdown cells with CHIKV at an MOI of 1 for 24 h, collected the cell supernatant for plaque assay analysis and harvested the total cells for RNA or protein analysis. Consistent with the drug inhibition of HSP-90, siRNA silencing of HSP-90 transcript showed a dramatic reduction in virus production (Fig. 3A), viral RNA (Fig. 3B) and viral protein levels (Fig. 3C), compared to the non-targeted siRNA infection control (Fig. 3). Despite the differing levels of HSP-90 mRNA knockdown with both specific siRNAs, a significant reduction in the CHIKV replication was observed (Fig. 3). Overall siRNA knockdown data here support the HSP-90 specific drug inhibition of CHIKV infection and suggest that HSP-90 has a critical function in CHIKV replication.

3.4. CHIKV nsP3 or nsP4 proteins interact with HSP-90β or HSP-90α subunits

With an aim to explore the mechanism of HSP-90 function during CHIKV replication, we used our previously described GFP-tagged CHIKV protein expressing constructs (Rathore et al., 2013). Based on the results shown above in Figs. 1 and 3, we hypothesized that HSP-90 protein must interact with the CHIKV non-structural proteins to help virus replication. To prove this, we over-expressed each of the GFP-CHIKV non-structural proteins for 24 h followed by fluorescent confocal microscopy imaging using antibody against total HSP-90 protein. Interestingly, two of the CHIKV nsPs (nsP3 and nsP4) showed strong co-localization with HSP-90 protein (Fig. 4A). Visually, nsP2 also appeared to show some degree of co-localization (Fig. 4A); however, this interaction was not validated by the GFP-pull-down assay that we performed. Indeed, despite the similar levels of expression of CHIKV nsP2 and nsP4 in our pull-down experiment, we did not observe any biochemical interaction between nsP2 and HSP-90. This suggests that the observed interaction with nsP4 is specific (Fig. 4B). Moreover, our data shows strong evidence of a novel, unreported, interaction between CHIKV nsP3 and HSP-90 protein (Fig. 4A). To further confirm the visual association of HSP-90 with CHKV proteins, we addressed the question whether HSP-90 protein could be pulled down along with the over-expressed GFP-CHIKV nsPs using an anti-GFP antibody. Indeed, in our pull-down assay we show strong and specific interactions between CHIKV nsP3 or nsP4 proteins and HSP-90 (Fig. 4B). These studies investigated the role of total HSP-90 protein during CHIKV infection; however, HSP-90 protein in a mammalian cell exists in two isomeric forms; a cytoplasmic HSP-90α subunit and an ER predominant HSP-90β subunit (Little et al., 1994; Meng et al., 1996). Therefore, we sought to investigate whether there is any specificity in interaction between CHIKV nsP3 or nsP4 proteins with HSP-90α or HSP-90β subunits. For this, we over-expressed CHIKV nsP3, nsP4 or GFP-only in HEK-293T cells for 24 h followed by GFP pull-downs using GFP-TrapA beads. The pull-down samples were run on SDS–PAGE and silver stained. We observed minimal background interaction with GFP, yet many interacting bands were seen in CHIKV nsP3 or nsP4 pull-down lanes (Fig. 4C). Further analysis of these pull-down samples using LC/ESI/MS/MS mass-spectrometry revealed unique specific interactions between CHIKV GFP-nsP3 with HSP-90β subunit (17 unique peptides matched) or GFP-nsP4 with HSP-90α and HSP-90β subunits, respectively (16 or 13 unique peptides matched, respectively). GFP alone as a control did not show any significant interaction with either HSP-90α or HSP-90β subunits (only 1 or 0 unique peptides matched, respectively) (Figs. 4D and S2). This data suggests that nsP3 may interact more specifically with HSP-90β while nsP4 may interact with both HSP-90α and HSP-90β subunits (Figs. 4D and S2). Next to further verify our mass-spectrometry data we probed the GFP-pull-down samples with specific HSP-90α and HSP-90β antibodies by Western blotting. Consistent with our mass-spectrometry interaction data, we saw HSP-90α co-precipitated with over-expressed nsp4 while HSP-90β co-precipitated with over-expressed nsP3. GFP as a control did not precipitate either of the HSP-90 subunits (Fig. S3A). This specific interaction between HSP-90α and CHIKV-nsP4 could also be visualized using immunofluorescence confocal imaging (Fig. S3B). To address the significance of these interactions in the context viral infection, we did the reverse pull-downs using antibodies specific to HSP-90α and HSP-90β subunits and probed the western blots with anti-CHIKV-nsP3 and anti-CHIKV nsP4 polyclonal serum (Fig. 4E). Indeed, our data show that CHIKV-nsP3 co-precipitated with HSP-90β and CHIKV-nsP4 co-precipitated with HSP-90αproteins (Fig. 4E), thus validating all of the data obtained above through an over-expression system.

The importance of these specific interactions with unique HSP-90 subunits was further studied by specifically amplifying both HSP-90α and HSP-90β in the HSP-90 knockdown cells using siRNAs. By amplifying HSP-90α and HSP-90β transcripts separately we observed that siRNA(1) moderately silenced both the HSP-90α and HSP-90β subunits (Figs. 4F and S4). However, in the case of siRNA(2), only HSP-90α transcript was suppressed and not the HSP-90β, suggesting that siRNA(2) was specific to HSP-90α subunit (Figs. 4F and S4). Next, we dissected the roles of each individual HSP-90 subunit during CHIKV replication, using the specifically targeting siRNAs. Interestingly the amount of viral RNA produced was significantly reduced in the presence of siRNA(2) where HSP-90α subunit was knocked-down; however, the levels of HSP-90β subunit were not altered (Figs. 4F and S4). The data here

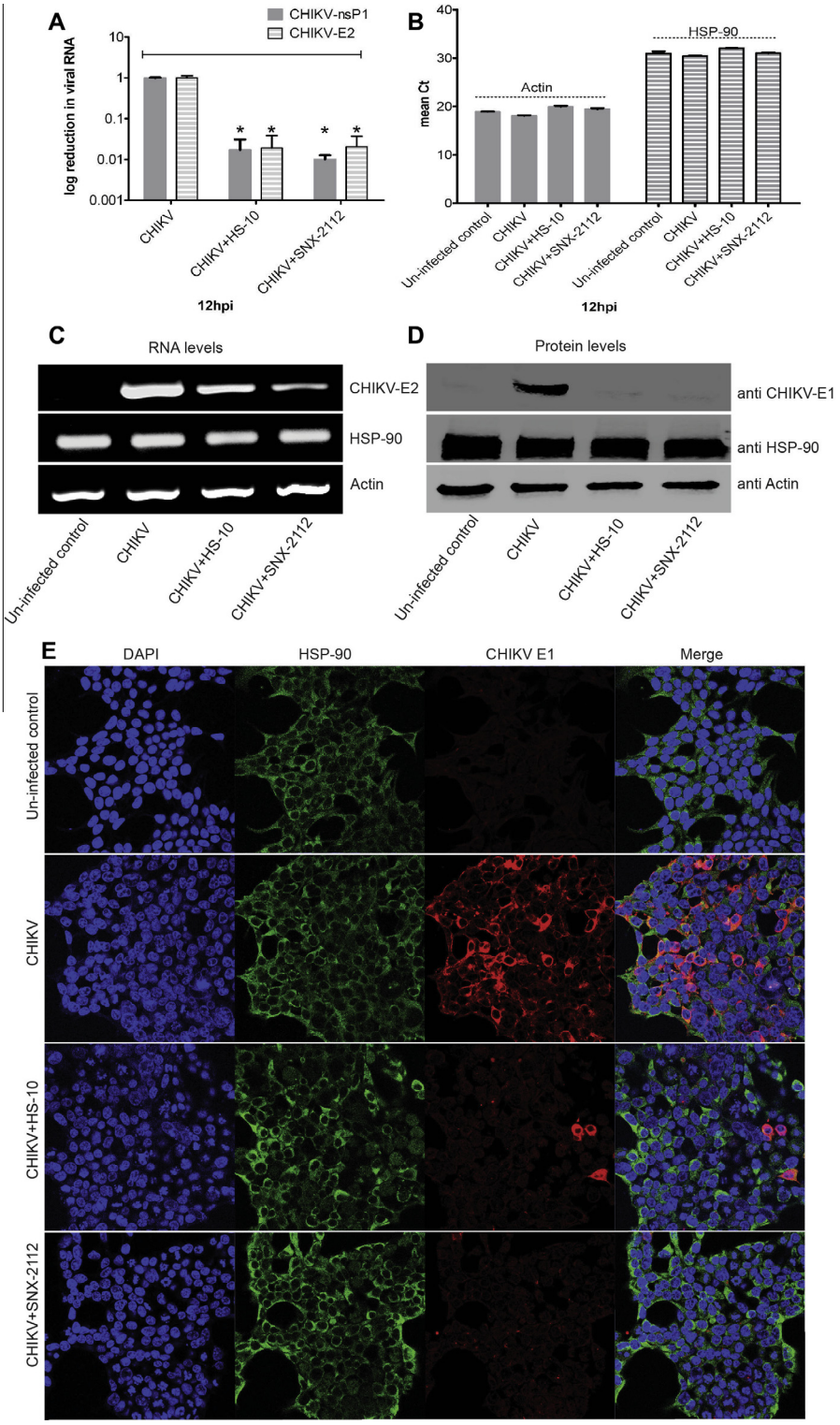

Fig. 2. CHIKV replication is affected by HSP-90 inhibitors. (A) Real time PCR analysis of viral nsP1 or E2 and host HSP-90 (total) gene from the total RNA extracted from the CHIKV-infected (MOI-1) cells, which were either mock or HS-10 or SNX-2112 treated at the dose of 10 μM for 12 h show reduction in the viral RNA after normalization to the levels seen in the infected but untreated control and actin. The reduction in viral RNA is highly significant as determined by one-way ANOVA test (p = <0.0001). (B) Mean Ct values from the Real time RT PCR are presented to show that drug treatments had no effects on the mRNA levels of total HSP-90. (C) Real time PCR products were run on 2% agarose gel to verify the correct amplification sizes of each of the CHIKV E2, HSP-90 and actin transcripts. (D) Under similar experimental conditions as described above, Western blotting was performed using antibodies specific for total HSP-90 and CHIKV E protein. Uninfected/untreated cells and mock-treated but infected (CHIKV) cells are shown as endogenous controls and actin was used as the input RNA or loading control. (E) Immunofluorescence microscopy images show significant reduction in CHIKV replication (CHIKV E protein-red) upon treatment with either HS-10 or SNX-2112. Endogenous levels of total HSP-90 are shown in green whereas the nucleus is stained blue. HEK-293T cells were grown overnight on a tissue culture coverslip in a 24-well plate followed by 1 h infection with CHIKV at an MOI of 1. After infection, excess media was removed and cells were either mock or HS-10 or SNX-2112 treated at a dose of 2 μM, for 12 h. (For interpretation of the references to color in this figure legend, the reader is referred to the web version of this article.)

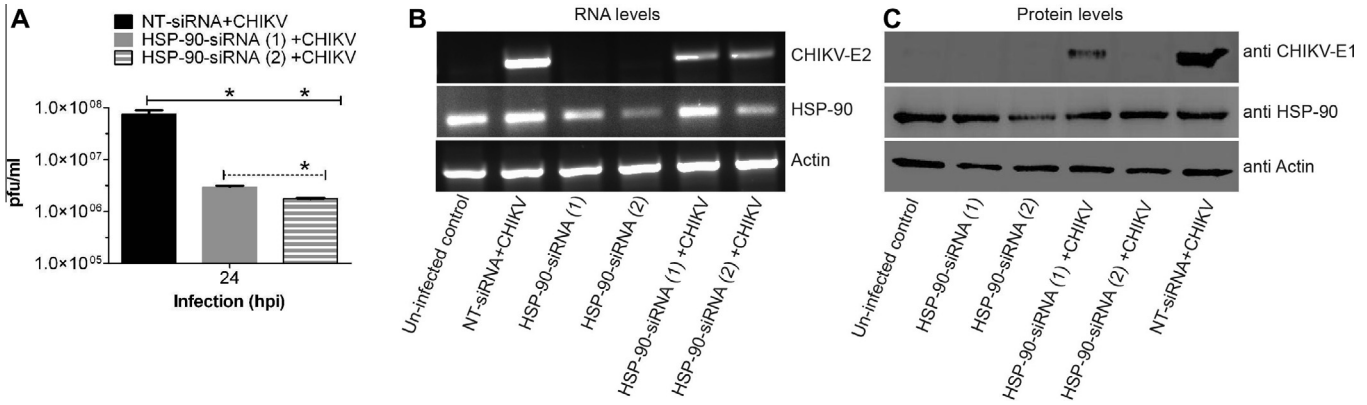

Fig. 3. siRNA knockdown of HSP-90 has deleterious effects on CHIKV replication. (A and B) HEK-293T cells were transfected with 100 nM of each of the siRNAs for 24 h followed by infection with CHIKV at MOI-1 for 24 h. At 24 h post infection, cells were harvested to check the efficiency of HSP-90 knockdowns and the media supernatants were collected for plaque assay analysis. (A) Plaque assay data shows reduced CHIKV titers in HSP-90 knockdown cells. (B and C) RT-PCR or Western blotting shows the total mRNA or protein levels of HSP-90 in each of the specific siRNA treated groups. During HSP-90 knockdown, the levels of both viral RNA (CHIKV-E2 gene) and protein (CHIKV-E protein) was significantly reduced as compared to the infected but non-targeted siRNA control group.

shows for the first time that in addition to HSP-90β, HSP-90α plays an essential role in CHIKV replication and that the interaction between CHIKV nsp4 and HSP-90α might be critical for assembly of the viral replication complex.

3.5. HSP-90 inhibitors reduce CHIKV viremia and inflammation in vivo

The specificity of the action of HSP-90-targeted drugs and the finding that specific biochemical interactions occur between HSP-90 subunits and viral nsPs, prompted us to evaluate the efficacy of these drugs in a CHIKV mouse model of lethal infection and inflammation. Mice (SvA129) deficient in type-I interferons (IFN-α and IFN-β) were infected with 100 pfu of a clinical isolate of CHIKV via the footpad route and either mock or HS-10 or SNX-2112 treated via *i.p.* injection at a dose of 10 mg/kg twice a day for 3 days. Serum viremia levels on day 2 (~48 h) in the treated group showed significant reduction in the virus titers compared to the mock-treated group (Fig. 5A). Viral infection was also probed in the limb muscle using RT-PCR at 24, 48, and 72 h from the animals that were either mock or SNX-2112 treated (Fig. S5). Consistent with the viremia data we show that at 24 and 48 h post infection, viral burden in the muscle of animals treated with SNX-2112 was significantly reduced compared to the untreated animals (Fig. S5). However since CHIKV infection of A129 mice is lethal, no difference in the level of viral RNA was observed between the mock and treated animals at 72 h post infection (Fig. S5). Next, to determine the effects of the drug treatments on inflammation, we harvested the muscle tissues from animals from each group and processed them for cryo-sectioning followed by Hematoxylin and Eosin (H&E) staining. The cross-sections stained with H&E showed substantial infiltration of mononuclear cells and considerable tissue damage in mock-treated infected animals (Fig. 5B). However, muscle cross-sections from mice treated with either HS-10 or SNX2112 showed significant reduction in both the tissue damage and infiltration of mononuclear cells (Fig. 5B). The measurement of width and thickness of the limbs of infected animals treated with HS-10 or SNX-2112 showed that CHIKV induced inflammation is significantly reduced compared to the untreated animals (Figs. 5C and S6). To explore further, we measured the serum concentrations of selected cytokines such as IL-6, IL-12, IFN-γ, and TNF-α, which have been associated with inflammation during CHIKV infection (Hoarau et al., 2010). Our data showed that the serum cytokine levels of IL-12 and IFN- γ were significantly reduced upon treatment with HS-10 or SNX-2112 when compared to the levels in mock-treated infected animals (Fig. 5D). On the other hand the levels of IL-6 and TNF-α, were higher in the SNX-2112 treated animals compared to untreated or HS-10 treatment (Fig. 5D).

4. Discussion

Small RNA viruses such as CHIKV must rely on the host cellular machinery to complete the viral life cycle, which includes folding and maturation of viral proteins by host chaperones. Drugs targeting these host cellular factors provide an added advantage over the conventional approach of directly targeting viral proteins that usually results in rapid acquisition of drug resistance by viruses. The protein homeostasis in a cell is monitored by the UPR that functions through the use of several signaling and chaperone proteins, including HSP-90. Our previous study has shown the relevance of UPR during CHIKV infection and revealed the key interplay of viral nsP4 in modulating the host UPR machinery (Rathore et al., 2013). HSP-90 has been shown to facilitate various aspects of virus replication during many viral infections. In this study we show that the drugs targeting HSP-90 have profound effects on CHIKV replication. HSP-90 is a highly druggable target and to date many structurally diverse pharmacological inhibitors have been identified. The majority of these inhibitors block the ATP binding site in the HSP-90 protein. Both the inhibitors used in this study, HS-10 and SNX-2112, reduced CHIKV infection in a dose-dependent manner. Indeed, real time RT-PCR amplification of viral specific nsP1 or E2 genes confirmed the effect of these inhibitors on CHIKV replication. Treatment of cells with HS-10 or SNX-2112 showed significant reduction of viral RNA as early as 6 h post infection (data not shown) or protein levels at 12 h post infection suggesting the effects of HS-10 and SNX-2112 at the virus replication level. To further understand the importance of HSP-90 during CHIKV replication, we silenced HSP-90 mRNA using two different siRNAs targeting different sites in the gene. Interestingly, a dramatic reduction in the virus replication both at the RNA and protein level was observed upon siRNA knockdown of HSP-90 gene, implicating the critical role of HSP-90 during CHIKV replication. Next, to understand the detailed function of HSP-90 during CHIKV replication we hypothesized that viral non-structural proteins must interact with the HSP-90 protein to complete its function in the viral replication cycle. By over-expressing each of the CHIKV non-structural proteins followed by co-immunoprecipitation or by using confocal microscopy we showed that CHIKV nsP4 physically inter-

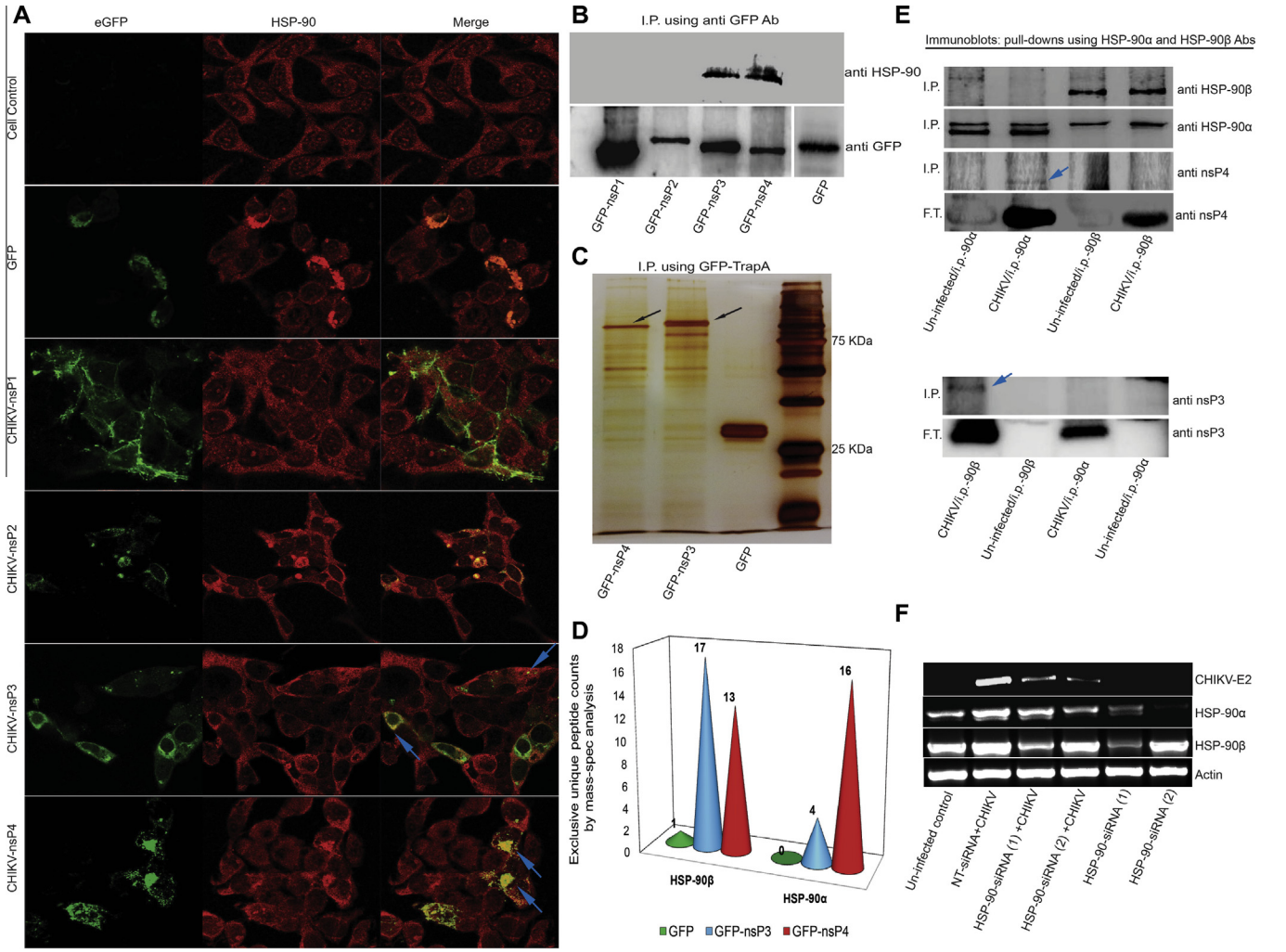

Fig. 4. Interactions between CHIKV nsP3 and nsP4 with HSP-90 subunits. (A) Co-localization (yellow) of CHIKV nsP3 and nsP4 proteins (green) with the HSP-90 protein (red). GFP alone, CHIKV nsP1 and nsP2 show some degree of laser channel bleed-through (orange) with no obvious co-localization with the HSP-90 protein. For co-localization studies, HEK-293T cells were grown on tissue culture coverslips and transfected with 1 μg of each of the GFP-fused CHIKV non-structural gene plasmids. After 24 h post-transfection cells were fixed with 80% acetone and blocked with 2% fish gelatin overnight at 4 °C, followed by staining with HSP-90 antibody. Images were captured using a Zeiss Confocal Microscope at 63× magnification. (B) Pull-down of GFP-fused CHIKV non-structural proteins and detection of HSP-90 shows the co-immunoprecipitation of HSP-90 protein together with CHIKV nsP3 and nsP4 proteins. Briefly, GFP only and GFP-fused CHIKV non-structural proteins were allowed to express in HEK-293T cells for 24 h. At 24 h post transfection cells were lysed in the TNET lysis buffer containing complete protease inhibitor cocktail and co-immunoprecipitations with 2 μg of anti-GFP antibody was carried out as described in Section 2. (C) Silver stained gel of an aliquot after GFP-nsP3 or GFP-nsP4 pull-down using GFP-TrapA beads for mass-spectrometric analysis shows several unique host protein bands. See Section 2. (D) Graphical illustration of the number of unique peptides matched for HSP-90α or β with GFP only, nsP3 or nsP4 pull-downs. LC/ESI/MS/MS mass-spectrometric analysis of GFP pull-down samples revealed specific interactions between nsP4 and HSP-90α/β subunit or GFP-nsP3 and HSP-90β subunit. GFP on its own did not show any interaction with either of the HSP-90 subunits. See Section 2. (E) Western blot showing that CHIKV-nsP3 co-immunoprecipitates with HSP-90β and CHIKV-nsP4 co-immunoprecipitates with HSP-90α. For immunoprecipitation, HEK-293T cells were infected with CHIKV-ROSS at MOI-1 for 24 h followed by cell lysis and co-immunoprecipitation using antibodies specific to HSP-90α or β subunits as described in Materials and methods. Un-infected cell lysate immunoprecipitation was used as negative control and the flow-through samples after co-immunoprecipitation (F.T.) were run as infection positive controls. (F) CHIKV replication in HEK-293T cells following siRNA knockdown of HSP-90. The figure shows that the siRNA(1) moderately silenced both HSP-90α/β subunits and significantly reduced CHIKV replication as compared to the NT-siRNA control. However, in case of siRNA(2) only HSP-90α transcript was suppressed and not the HSP-90β, suggesting that siRNA(2) is specific to HSP-90α subunit. The amount of viral RNA produced in presence of siRNA(2) was much significantly reduced compared to both NT-siRNA control and siRNA(1), suggesting the critical role of HSP-90α subunit during CHIKV replication. Briefly, HEK-293T cells were transfected with 100 nM each of the siRNAs for 24 h, followed by infection of cells with CHIKV at an MOI-1 for 24 h. At 24 h post infection, total RNA was extracted using a Trizol extraction reagent and cDNA was synthesized using oligodT as primers. Equal amounts of cDNA (50 ng) were used for PCR amplification of CHIKV E2 (305 bp) and individual HSP-90α (2196 bp) or HSP-90β (2172 bp) subunits. Actin was used as an input RNA control. (For interpretation of the references to color in this figure legend, the reader is referred to the web version of this article.)

acts with HSP-90. Similar interaction has been shown for Sindbis virus using Flag-tagged protein and also by yeast-2-hybrid interaction analysis (Bourai et al., 2012; Cristea et al., 2010). Very interestingly, using our co-immunoprecipitation system we identified CHIKV nsP3 as a novel interacting partner of HSP-90 protein. The specificity in interactions between nsp3 and HSP-90β or nsP4 and HSP-90α shown using over-expression system as well as in viral infection system along with the mass-spectrometry data and siRNA knockdown experiments, suggest an integral role for these interactions during CHIKV replication. Since HSP-90α is predominantly cytosolic (Lees-Miller and Anderson, 1989), it may help in stabilization of CHIKV nsP4 and formation of the CHIKV replication complex (Strauss and Strauss, 1994). This notion is supported by the siRNA knockdown of HSP-90α subunit that resulted in greater inhibition of viral replication than targeting theHSP-90β subunit. Overall the current data implicates a pivotal role for HSP-90α and a possible ancillary role for HSP-90β subunits in facilitating CHIKV replication. However, further detailed studies are warranted to clearly show the involvement of HSP-90α or HSP-90β in a CHIKV replication complex. Since, the alphavirus

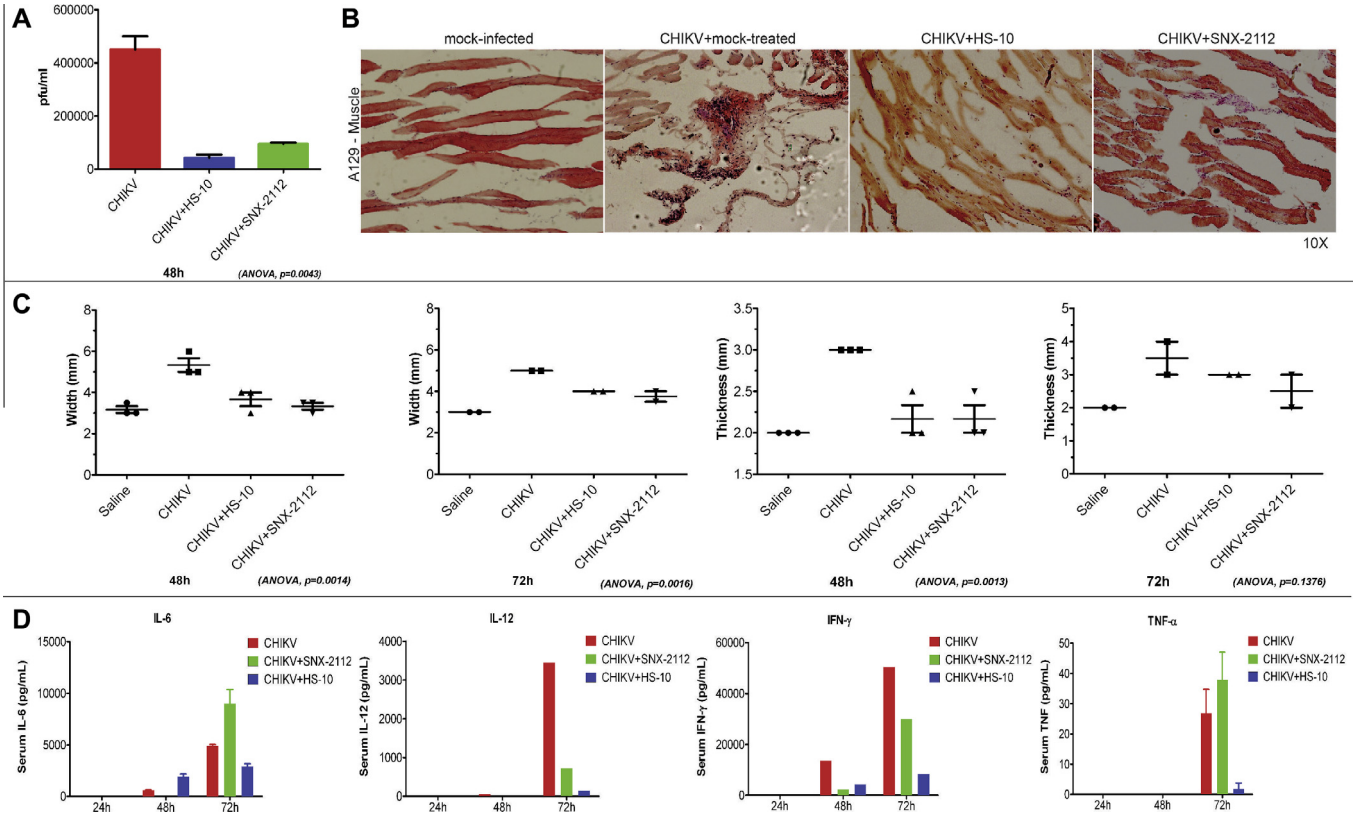

Fig. 5. *In vivo* testing of HSP-90 inhibitors in a lethal mouse model of CHIKV infection. (A) The serum viral load in CHIKV infected mice (SvA129, $n = 6$) at 48 h post infection was significantly reduced upon treatment with HS-10 or SNX-2112. Mice (SvA129, $n = 6$) were infected with 100 pfu of a clinical isolate of CHIKV via the footpad route and either mock or HS-10 or SNX-2112 treated (10 mg/kg twice a day) for 3 days. (B) H&E stained cross-section of limb muscle obtained from CHIKV infected mice (as above) at day 3. Muscle cross-section from mock treated but infected mice showed extensive infiltration of mononuclear cells and tissue damage, which is reflective of tissue inflammation. Treatment with either HS-10 or SNX-2112 showed dramatic reduction in tissue damage as well as mononuclear cell infiltrations. (C) Measurement of swelling (thickness and width of the limb, as depicted in Fig. S6) in infected limbs at 48 and 72 h with or without treatment with HS-10 or SNX-2112 indicates that the drugs reduce swelling and inflammation caused by CHIKV infection in this mouse model. (D) ELISA quantification of pro-inflammatory cytokines such as IL-6, IL-12, IFN-γ, and TNF-α in the serum of CHIKV infected/treated mice. The levels of some of these pro-inflammatory cytokines such as IL-12 and IFN-γ were significantly reduced during HS-10 or SNX-2112 treatment.

replication complex is shown to involve several host proteins as revealed by extensive studies in Semliki Forest virus and Sindbis virus infections (Cristea et al., 2010; Varjak et al., 2013), the role of HSP-90 in CHIKV replication is firmly anticipated.

Having shown the effectiveness of HSP-90 targeting drugs in cell culture and also understanding the mechanism of HSP-90 during CHIKV replication, we sought to evaluate the efficacy of HSP-90 inhibitor drugs in an *in vivo* infection model. We chose to use the IFN-deficient animals to facilitate maximal CHIKV replication *in vivo*. Both the drugs HS-10 and SNX-2112 significantly reduced viral titers on day 2 (~48 h). However, viremia in all the animals further increased to the levels of untreated control group on day 3 (~72 h) (data not shown), likely due to the lack of any IFN response in these animals. Nevertheless, unlike untreated CHIKV infected mice, all the animals treated with either HS-10 or SNX-2112 never developed swelling or inflammation during the course of infection. Further studies using microscopic visualizations of cross-sections of muscle tissues and by measuring the serum concentrations of pro-inflammatory cytokines (IL-6, IL-12, IFN-γ, and TNF-α) clearly demonstrated the ability of these drugs to suppress the CHIKV-induced inflammation in mice. Increased suppression in the levels of some of these inflammatory cytokines in our severe immune-compromised animals could also explain why the viral titers in the treated animals were increased at day 3, aside from the direct role of IFN on viral clearance. All in all, in this study we have shown the importance of HSP-90 protein during CHIKV replication and, indeed, drugs targeting HSP-90 could significantly reduce CHIKV infection or inflammation. The precise mechanism of interaction and the immuno modulatory mechanisms remain to be teased out in detail in studies that are currently underway.

Conflict of interest

The authors ascertain that they do not have any commercial interest or other associations with this work that might pose a potential conflict of interest.

Acknowledgements

We thank Dr. Ooi Eng Eong for providing the clinical isolate of CHIKV. We thank Drs. Ashley St. John and Satoru Watanabe for critical reading and providing in-depth discussion on the manuscript. We also thank Dr. Arthur Moseley for help in mass-spectrometry data acquisition and analysis. This work is supported by the start up funds to S.G.V. from Duke-NUS signature research program funded by the Agency for Science, Technology and Research, Singapore and the Ministry of Health, Singapore.

Appendix A. Supplementary data

Supplementary data associated with this article can be found, in the online version, at http://dx.doi.org/10.1016/j.antiviral.2013.12.010.

References

Ali, M.M., Roe, S.M., Vaughan, C.K., Meyer, P., Panaretou, B., Piper, P.W., Prodromou, C., Pearl, L.H., 2006. Crystal structure of an Hsp90-nucleotide-p23/Sba1 closed chaperone complex. Nature 440, 1013–1017.

Bodnar, W.M., Blackburn, R.K., Krise, J.M., Moseley, M.A., 2003. Exploiting the complementary nature of LC/MALDI/MS/MS and LC/ESI/MS/MS for increased proteome coverage. J. Am. Soc. Mass Spectrom. 14, 971–979.

Borgherini, G., Poubeau, P., Staikowsky, F., Lory, M., Le Moullec, N., Becquart, J.P., Wengling, C., Michault, A., Paganin, F., 2007. Outbreak of Chikungunya on Reunion Island: early clinical and laboratory features in 157 adult patients. Clin. Infect. Dis. 44, 1401–1407.

Bourai, M., Lucas-Hourani, M., Gad, H.H., Drosten, C., Jacob, Y., Tafforeau, L., Cassonnet, P., Jones, L.M., Judith, D., Couderc, T., Lecuit, M., Andre, P., Kummerer, B.M., Lotteau, V., Despres, P., Tangy, F., Vidalain, P.O., 2012. Mapping of Chikungunya virus interactions with host proteins identified nsP2 as a highly connected viral component. J. Virol. 86, 3121–3134.

Burt, F.J., Rolph, M.S., Rulli, N.E., Mahalingam, S., Heise, M.T., 2012. Chikungunya: a re-emerging virus. Lancet 379, 662–671.

Chadli, A., Bouhouche, I., Sullivan, W., Stensgard, B., McMahon, N., Catelli, M.G., Toft, D.O., 2000. Dimerization and N-terminal domain proximity underlie the function of the molecular chaperone heat shock protein 90. Proc. Natl. Acad. Sci. USA 97, 12524–12529.

Chen, B., Piel, W.H., Gui, L., Bruford, E., Monteiro, A., 2005. The HSP90 family of genes in the human genome: insights into their divergence and evolution. Genomics 86, 627–637.

Cristea, I.M., Rozjabek, H., Molloy, K.R., Karki, S., White, L.L., Rice, C.M., Rout, M.P., Chait, B.T., MacDonald, M.R., 2010. Host factors associated with the Sindbis virus RNA-dependent RNA polymerase: role for G3BP1 and G3BP2 in virus replication. J. Virol. 84, 6720–6732.

Fadden, P., Huang, K.H., Veal, J.M., Steed, P.M., Barabasz, A.F., Foley, B., Hu, M., Partridge, J.M., Rice, J., Scott, A., Dubois, L.G., Freed, T.A., Silinski, M.A., Barta, T.E., Hughes, P.F., Ommen, A., Ma, W., Smith, E.D., Spangenberg, A.W., Eaves, J., Hanson, G.J., Hinkley, L., Jenks, M., Lewis, M., Otto, J., Pronk, G.J., Verleysen, K., Haystead, T.A., Hall, S.E., 2010. Application of chemoproteomics to drug discovery: identification of a clinical candidate targeting hsp90. Chem. Biol. 17, 686–694.

Geller, R., Taguwa, S., Frydman, J., 2012. Broad action of Hsp90 as a host chaperone required for viral replication. Biochim. Biophys. Acta 1823, 698–706.

Hoarau, J.J., Jaffar Bandjee, M.C., Krejbich Trotot, P., Das, T., Li-Pat-Yuen, G., Dassa, B., Denizot, M., Guichard, E., Ribera, A., Henni, T., Tallet, F., Moiton, M.P., Gauzere, B.A., Bruniquet, S., Jaffar Bandjee, Z., Morbidelli, P., Martigny, G., Jolivet, M., Gay, F., Grandadam, M., Tolou, H., Vieillard, V., Debre, P., Autran, B., Gasque, P., 2010. Persistent chronic inflammation and infection by Chikungunya arthritogenic alphavirus in spite of a robust host immune response. J. Immunol. 184, 5914–5927.

Hu, J., Anselmo, D., 2000. In vitro reconstitution of a functional duck hepatitis B virus reverse transcriptase: posttranslational activation by Hsp90. J. Virol. 74, 11447–11455.

Hu, J., Toft, D.O., Seeger, C., 1997. Hepadnavirus assembly and reverse transcription require a multi-component chaperone complex which is incorporated into nucleocapsids. EMBO J. 16, 59–68.

Huang, K.H., Veal, J.M., Fadden, R.P., Rice, J.W., Eaves, J., Strachan, J.P., Barabasz, A.F., Foley, B.E., Barta, T.E., Ma, W., Silinski, M.A., Hu, M., Partridge, J.M., Scott, A., DuBois, L.G., Freed, T., Steed, P.M., Ommen, A.J., Smith, E.D., Hughes, P.F., Woodward, A.R., Hanson, G.J., McCall, W.S., Markworth, C.J., Hinkley, L., Jenks, M., Geng, L., Lewis, M., Otto, J., Pronk, B., Verleysen, K., Hall, S.E., 2009. Discovery of novel 2-aminobenzamide inhibitors of heat shock protein 90 as potent, selective and orally active antitumor agents. J. Med. Chem. 52, 4288–4305.

Hughes, P.F., Barrott, J.J., Carlson, D.A., Loiselle, D.R., Speer, B.L., Bodoor, K., Rund, L.A., Haystead, T.A., 2012. A highly selective Hsp90 affinity chromatography resin with a cleavable linker. Bioorg. Med. Chem. 20, 3298–3305.

Kaur, P., Chu, J.J., 2013. Chikungunya virus: an update on antiviral development and challenges. Drug Discov. Today 18, 969–983.

Lees-Miller, S.P., Anderson, C.W., 1989. The human double-stranded DNA-activated protein kinase phosphorylates the 90-kDa heat-shock protein, hsp90 alpha at two NH2-terminal threonine residues. J. Biol. Chem. 264, 17275–17280.

Li, L., Jose, J., Xiang, Y., Kuhn, R.J., Rossmann, M.G., 2010. Structural changes of envelope proteins during alphavirus fusion. Nature 468, 705–708.

Little, E., Ramakrishnan, M., Roy, B., Gazit, G., Lee, A.S., 1994. The glucose-regulated proteins (GRP78 and GRP94): functions, gene regulation, and applications. Crit. Rev. Eukaryot. Gene Expr. 4, 1–18.

Lulla, V., Kim, D.Y., Frolova, E.I., Frolov, I., 2013. The amino-terminal domain of alphavirus capsid protein is dispensable for viral particle assembly, but regulates RNA encapsidation through cooperative function of its subdomains. J. Virol. 87, 12003–12019.

Meng, X., Devin, J., Sullivan, W.P., Toft, D., Baulieu, E.E., Catelli, M.G., 1996. Mutational analysis of Hsp90 alpha dimerization and subcellular localization: dimer disruption does not impede "in vivo" interaction with estrogen receptor. J. Cell Sci. 109 (Pt 7), 1677–1687.

Momose, F., Naito, T., Yano, K., Sugimoto, S., Morikawa, Y., Nagata, K., 2002. Identification of Hsp90 as a stimulatory host factor involved in influenza virus RNA synthesis. J. Biol. Chem. 277, 45306–45314.

Naito, T., Momose, F., Kawaguchi, A., Nagata, K., 2007. Involvement of Hsp90 in assembly and nuclear import of influenza virus RNA polymerase subunits. J. Virol. 81, 1339–1349.

Okamoto, T., Nishimura, Y., Ichimura, T., Suzuki, K., Miyamura, T., Suzuki, T., Moriishi, K., Matsuura, Y., 2006. Hepatitis C virus RNA replication is regulated by FKBP8 and Hsp90. EMBO J. 25, 5015–5025.

Pearl, L.H., Prodromou, C., 2006. Structure and mechanism of the Hsp90 molecular chaperone machinery. Annu. Rev. Biochem. 75, 271–294.

Prodromou, C., Panaretou, B., Chohan, S., Siligardi, G., O'Brien, R., Ladbury, J.E., Roe, S.M., Piper, P.W., Pearl, L.H., 2000. The ATPase cycle of Hsp90 drives a molecular 'clamp' via transient dimerization of the N-terminal domains. EMBO J. 19, 4383–4392.

Rashad, A.A., Mahalingam, S., Keller, P.A., 2013. Chikungunya virus: emerging targets and new opportunities for medicinal chemistry. J. Med. Chem..

Rathore, A.P., Ng, M.L., Vasudevan, S.G., 2013. Differential unfolded protein response during Chikungunya and Sindbis virus infection: CHIKV nsP4 suppresses eIF2alpha phosphorylation. Virol. J. 10, 36.

Rathore, A.P., Paradkar, P.N., Watanabe, S., Tan, K.H., Sung, C., Connolly, J.E., Low, J., Ooi, E.E., Vasudevan, S.G., 2011. Celgosivir treatment misfolds dengue virus NS1 protein, induces cellular pro-survival genes and protects against lethal challenge mouse model. Antiviral Res. 92, 453–460.

Schwartz, O., Albert, M.L., 2010. Biology and pathogenesis of Chikungunya virus. Nat. Rev. Microbiol. 8, 491–500.

Stebbins, C.E., Russo, A.A., Schneider, C., Rosen, N., Hartl, F.U., Pavletich, N.P., 1997. Crystal structure of an Hsp90–geldanamycin complex: targeting of a protein chaperone by an antitumor agent. Cell 89, 239–250.

Strauss, J.H., Strauss, E.G., 1994. The alphaviruses: gene expression, replication, and evolution. Microbiol. Rev. 58, 491–562.

Varjak, M., Saul, S., Arike, L., Lulla, A., Peil, L., Merits, A., 2013. Magnetic fractionation and proteomic dissection of cellular organelles occupied by the late replication complexes of semliki forest virus. J. Virol. 87, 10295–10312.

Voss, J.E., Vaney, M.C., Duquerroy, S., Vonrhein, C., Girard-Blanc, C., Crublet, E., Thompson, A., Bricogne, G., Rey, F.A., 2010. Glycoprotein organization of Chikungunya virus particles revealed by X-ray crystallography. Nature 468, 709–712.